

Acoustic resonance spectroscopy for the advanced undergraduate laboratory

This article has been downloaded from IOPscience. Please scroll down to see the full text article.

2012 Eur. J. Phys. 33 1761

(<http://iopscience.iop.org/0143-0807/33/6/1761>)

View [the table of contents for this issue](#), or go to the [journal homepage](#) for more

Download details:

IP Address: 137.112.34.173

The article was downloaded on 17/11/2012 at 18:15

Please note that [terms and conditions apply](#).

Acoustic resonance spectroscopy for the advanced undergraduate laboratory

J A Franco-Villafañe¹, E Flores-Olmedo², G Báez²,
O Gandarilla-Carrillo³ and R A Méndez-Sánchez¹

¹ Instituto de Ciencias Físicas, Universidad Nacional Autónoma de México, PO Box 48-3, 62251 Cuernavaca, Morelos, Mexico

² Departamento de Ciencias Básicas, Universidad Autónoma Metropolitana-Azcapotzalco, Av San Pablo 180, Col Reynosa Tamaulipas, 02200 México DF, Mexico

³ Departamento de Ingeniería Eléctrica, Universidad Autónoma Metropolitana-Iztapalapa, AP 55-534, 09340 México DF, Mexico

E-mail: mendez@fis.unam.mx

Received 26 June 2012, in final form 7 September 2012

Published 3 October 2012

Online at stacks.iop.org/EJP/33/1761

Abstract

We present a simple experiment that allows advanced undergraduates to learn the principles and applications of spectroscopy. The technique, known as *acoustic resonance spectroscopy*, is applied to study a vibrating rod. The setup includes electromagnetic-acoustic transducers, an audio amplifier and a vector network analyzer. Typical results of compressional, torsional and bending waves are analyzed and compared with analytical results.

(Some figures may appear in colour only in the online journal)

1. Introduction

Spectroscopy is a broad-field experimental technique in physics with many applications. Historically, spectroscopy was crucial in developing quantum mechanics, one of the fundamental pillars of physics. Spectroscopy is now a tool used in research laboratories across the world in physics, chemistry and biology, and it should be introduced to physics students at an advanced stage of their education. For this reason we have designed an experiment for an advanced—third year—undergraduate physics laboratory, based on acoustic resonance spectroscopy (ARS). This spectroscopy involves scattering of acoustic and mechanical waves; the former for longitudinal (pressure) waves and the latter for transverse waves, among others. Compared with other spectroscopic techniques, ARS is a non-destructive technique that requires minimal sample preparation. The sample used here is a uniform rod of circular cross-section that can be changed easily by beams or plates that are uniform or structured for some specific purpose. Another advantage is that the ARS results can be analyzed in depth and compared with theoretical predictions.

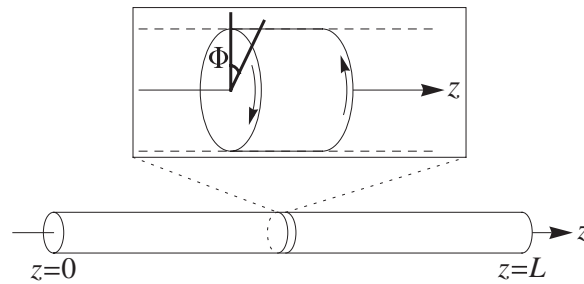


Figure 1. Uniform rod with circular cross-section. In the close-up the angle of twist Φ is defined. The arrows indicate the torque.

In this paper ARS is presented using a very simple system: a vibrating rod. In the next section we present the resonant response theory of torsional waves in a rod. In section 3 we present ARS as well as the experimental setup with a description of the transducers used. A comparison between theory and experiment is performed in section 4. A brief conclusion follows.

2. Theory: resonances with losses for torsional waves in rods

A vibrating rod at low frequencies is one of the simplest cases for studying elastic systems. In this regime elastic rods can vibrate in three different ways: compressional, torsional and bending [1–3]; an illustrative animation of these vibrations can be found in [4]. At low amplitudes, and for rods with circular cross-section, it is possible to study those different kinds of wave separately. In what follows we present the theory for torsional vibrations in rods that satisfy the wave equation. The compressional waves, in a first approximation, also satisfy the wave equation while bending (also called flexural) waves satisfy a fourth order partial differential equation [2, 5]. The theory developed below can be easily adapted, without major effort, to compressional and bending waves.

The torsional vibrations in rods with circular uniform cross-section (see figure 1) satisfy

$$\frac{\partial^2 \Phi}{\partial z^2} - \frac{1}{v^2} \frac{\partial^2 \Phi}{\partial t^2} = 0, \quad (1)$$

where Φ is the angle of twist, $v = \sqrt{G/\rho}$ is the speed of the torsional waves with G the shear modulus and ρ the density of the rod. To obtain the results for compressional waves, one has to change Φ by the longitudinal displacement u in the previous equation and use the speed of compressional waves $\sqrt{E/\rho}$ with E the Young modulus. Since the rod is free at one of its ends ($z = 0$), it satisfies the following boundary condition

$$\left. \frac{\partial \Phi}{\partial z} \right|_{z=0} = 0. \quad (2)$$

At the other end of the rod ($z = L$), a sinusoidal excitation of intensity F_0 and angular frequency ω is applied,

$$\left. \frac{\partial \Phi}{\partial z} \right|_{z=L} = F_0 \exp(i\omega t), \quad (3)$$

where F_0 is the ratio between the applied torque and the torsional rigidity [2]. Using separation of variables

$$\Phi(z, t) = \phi(z) \exp(i\omega t), \quad (4)$$

equation (1) can be written as

$$\frac{d^2\phi}{dz^2} + \frac{\omega^2}{v^2}\phi = 0, \quad (5)$$

with solution

$$\phi(z) = a \exp(ikz) + b \exp(-ikz). \quad (6)$$

Here $k = \omega/v$ is the wavenumber and $\phi(z)$ is the time independent angle of twist. The constants a and b can be evaluated as follows. From the boundary condition (2) one gets

$$\left. \frac{d\phi}{dz} \right|_{z=0} = ik(a - b) = 0, \quad (7)$$

i.e. $a = b$. Moreover, using (3) one gets

$$\phi(z) = -\frac{F_0}{k \sin(kL)} \cos(kz). \quad (8)$$

From the last equation it is possible to see that the angle of twist $\phi(z)$ goes to infinity when $\sin(kL) = 0$, i.e., when $kL = n\pi$, $n \in \mathbb{Z}$. This yields an infinite number of solutions, $k_n = n\pi/L$, that correspond to the normal mode frequencies

$$f_n = \frac{nv}{2L}, \quad n = 1, 2, 3, \dots \quad (9)$$

To avoid indeterminacy in the response (8) it is usual to include some absorption (losses) in a phenomenological way. This can be done by adding an imaginary part to the wavenumber: $k = k_R + ik_I$ where k_R and k_I are the real and imaginary parts of k , respectively. The imaginary part of the wavenumber is a parameter that fixes the intensity of the absorption. In general, k_I depends on the frequency in a very complicated way [6] and cannot be taken as a constant for the complete frequency range. In consequence, the angle of twist becomes complex. The response of the rod with absorption is then

$$\phi(z) = -\frac{F_0}{k} \left[\frac{\cos(k_R z) \cosh(k_I z) - i \sin(k_R z) \sinh(k_I z)}{\sin(k_R L) \cosh(k_I L) + i \cos(k_R L) \sinh(k_I L)} \right]. \quad (10)$$

For $z = 0$ the intensity of the response is

$$|\phi(z=0)|^2 = \frac{F_0^2}{(k_R^2 + k_I^2)[\sin^2(k_R L) + \sinh^2(k_I L)]}. \quad (11)$$

Now we will show that equation (11), near to the resonances, can be written in a Breit–Wigner (Lorentzian) form. This is called the *isolated resonances regime*. When $k_R L = n\pi + \delta$ with $\delta \ll 1$, i.e. close to the resonances, and for small absorption, i.e. $k_I L \ll 1$, equation (11) reduces to

$$|\phi(z=0)|^2 \approx A_n \frac{\Gamma/2}{(f - f_n)^2 + (\Gamma/2)^2}, \quad (12)$$

where $A_n = vF_0^2/2k_I n^2 \pi^3$ and $\Gamma = k_I v/\pi$. Here, f_n and Γ are the center and width of the resonance, respectively.

A plot of $|\phi(z=0)|^2$ as a function of $k_R L$ is given in figure 2(a) for two different values of the absorption intensity k_I . As can be seen in this figure, the intensity of the response shows peaks at $k_R L = n\pi$, with $n = 1, 2, 3, \dots$, which correspond to the normal modes. These peaks are usually called resonant. As can be seen in the figure, the height of the peaks decreases quadratically as a function of $k_R L$. Additionally, one can appreciate in the same figure that the width of the resonant peaks increases with k_I . This is only valid when the absorption parameter k_I is constant and if $k_I L \ll 1$; these assumptions are only true locally around the resonant frequencies. Thus, each resonant mode has a different k_I .

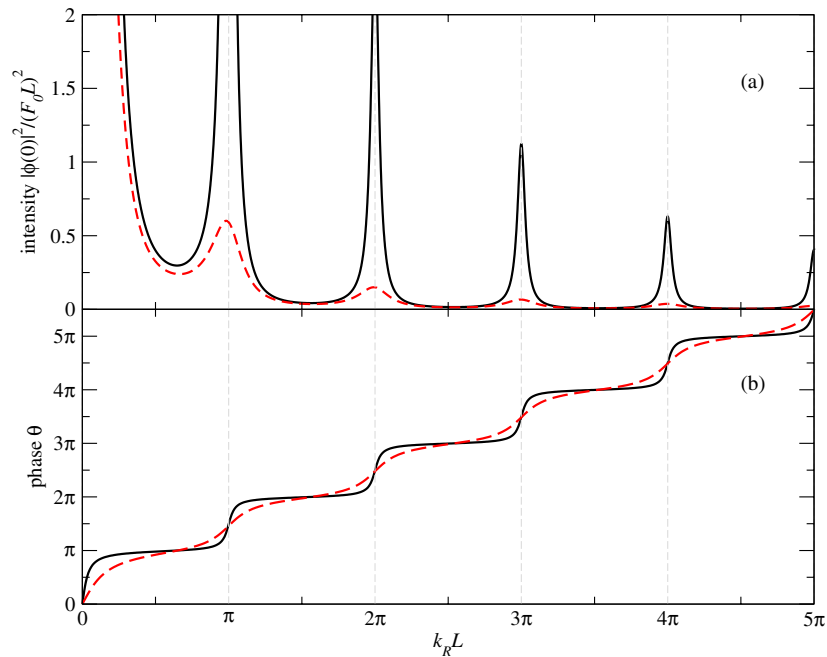


Figure 2. (a) Intensity $|\phi(z=0)|^2 / (F_0 L)^2$ of the angle of twist, equation (11), and (b) phase θ of the angle of twist, equation (13), as a function of $k_R L$. The continuous (black) lines correspond to $k_1 L = 0.1$ and the dashed (red online) lines correspond to $k_1 L = 0.4$.

As we see in the next section, the detector measures the acceleration of the metal surface. To obtain it, the expression (10) for the time independent angle of twist ϕ should be multiplied by ω^2 . Note that the Breit–Wigner result for the resonances (12) is still valid since it is assumed that the resonances are narrow ($\delta \ll 1$) and thus $f \approx f_n$.

In order to evaluate the phase of the resonance we write the angle of twist in polar form as $\phi(z=0) = |\phi(z=0)| \exp(i\theta)$, where

$$\tan \theta = -\frac{k_R \cos(k_R L) \sinh(k_1 L) + k_1 \sin(k_R L) \cosh(k_1 L)}{k_R \sin(k_R L) \cosh(k_1 L) - k_1 \cos(k_R L) \sinh(k_1 L)}. \quad (13)$$

A plot of the phase θ as a function of $k_R L$ is given in figure 2(b) for two different values of k_1 . Again, for isolated resonances it is possible obtain a simple expression for the phase:

$$\theta \approx \arctan\left(\frac{\Gamma/2}{f - f_n}\right). \quad (14)$$

From this equation one can see that the phase has a change of π for each resonance.

3. Experimental measurement of rod resonances

We use the experimental setup depicted in figure 3 to measure the resonances of an aluminum rod. As we see below, to excite and detect the vibrations, two electromagnetic-acoustic transducers (EMATs) are used [1, 3, 7]. The vector network analyzer (VNA) is the key component of the experimental setup of figure 3. A sinusoidal signal is generated by the VNA (ANRITSU model MS4630B) and sent to a high-fidelity Cerwin-Vega! audio amplifier (model CV900). The amplified signal is sent to the EMAT exciter located very close to one end ($z = L$)

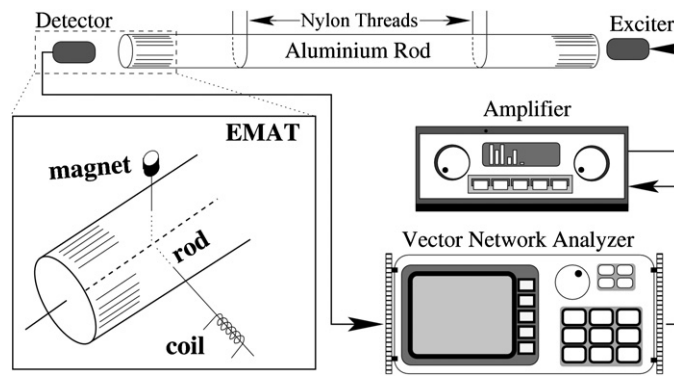


Figure 3. Experimental setup used to measure the resonant response of the aluminum rod. The EMAT (lower left corner) is configured to measure torsional waves. The rod is supported by two nylon threads.

of the rod. The exciter generates a sinusoidal torque on the aluminum rod (see equation (3)), which produces torsional waves of frequency f . A second EMAT measures the response at the free end of the rod ($z = 0$) and its signal is sent directly to the VNA. Although the range of frequency of the VNA can be swept from 10 Hz to 300 MHz, we work in a shorter range since the audio amplifier works only from 5 Hz to 60 kHz. The rod is supported by two nylon threads located at the nodes for the lower modes. The effect of this support is very small and decreases considerably for higher modes. To measure a spectrum without missing resonances it is important that both transducers are located close to the ends of the rod since the free boundary conditions guarantee a maximum amplitude for the vibration there. Note that moving the detector along the rod will give a measurement of the normal mode wave amplitude.

The EMATs can be built easily with coils and permanent magnets; changing the orientation of the coil and the magnet, with respect to the rod axis, different kinds of wave can be selectively excited or detected [1]. The EMATs are also invertible, i.e. they can be used as exciters or detectors. The configuration of the EMATs to excite (detect) the different kinds of waves in rods is shown in figure 4. Heuristically, the EMAT, as an exciter, operates as follows. A variable current $I(t)$ of frequency f in the coil generates a magnetic field oscillating with the same frequency. When a metal surface is near to the coil, due to Faraday's induction law eddy currents are produced in the metal. These currents interact with the EMAT's permanent magnet through the Lorentz force. In this way the surface is attracted and repelled at frequency f without mechanical contact. Heuristically, the EMAT, as a detector, works as follows. When a vibrating metallic surface is close to the EMAT's permanent magnet, the change of the flux of the magnetic field produces eddy currents on the metal proportional to the speed of the metal. These currents generate a magnetic field which induces an electromagnetic force proportional to the derivative of these currents on the EMAT's coil detector. Thus the detector measures the acceleration of the metal surface. Note that for each normal mode this is proportional to the amplitude of vibration since the frequency is almost constant.

In our experiment the EMAT exciter had a cylindrical neodymium magnet of 12 mm diameter, 12 mm height and 12000 G of residual induction and a coil with 100 turns, 40 mm diameter and 28 mm height. The enameled magnet wire used was no. 14 AWG. The EMAT detector had a cylindrical neodymium magnet of 4 mm diameter, 4 mm height and 12000 G of residual induction. The coil had 400 turns and 10 mm diameter and 10 mm

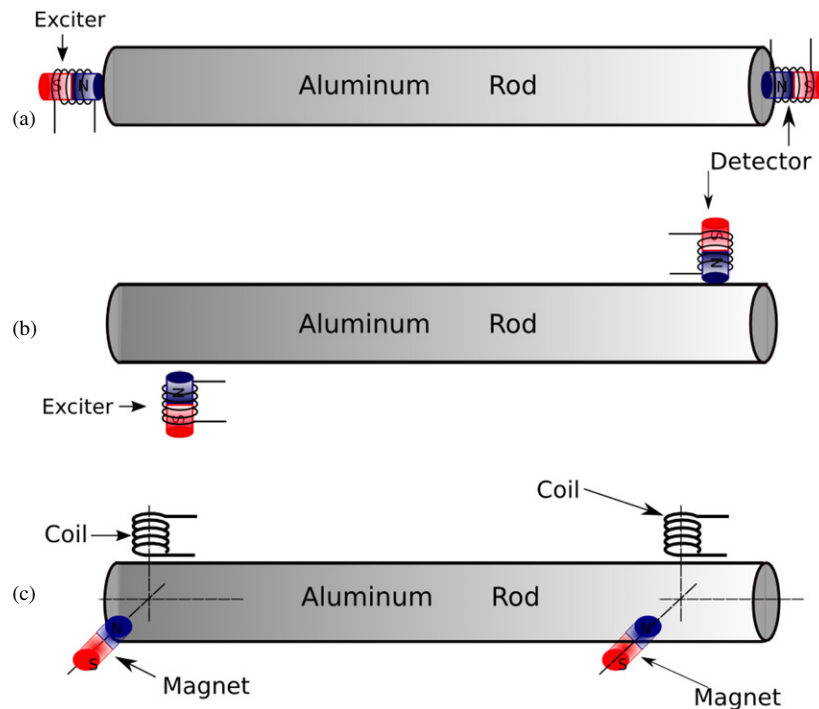


Figure 4. EMATs exciter/detector configurations to measure the different kinds of waves in rods: (a) compressional, (b) bending and (c) torsional.

height. The magnet wire in this case was no. 32 AWG. With these EMATs the power pumped into the EMAT exciter was of the order of 65 W, while the typical signal measured with the EMAT detector was of the order of 200 mV.

The exciter and detector are of finite size. Therefore, the interaction with the rod is not only at one point, as in the theoretical model of section 2, but in a finite region. This only affects the results when the wavelength is of the order of the size of the EMATs, which corresponds to modes with $n \gtrsim 100$ and yields a frequency that exceeds the maximum operating frequency of the amplifier.

The measurements made with the VNA can be transferred to a computer using a floppy disc or through a direct connection using the GPIB or RS-232 ports. The VNA allows measurement of both the intensity and the phase of the response.

4. Comparison between theory and experiment

In figure 5 we show the measured spectra, with the EMATs in the different configurations of figure 4. As can be seen, the different kinds of vibrations are selected by the EMATs, since different peaks appear for different configurations. Only a very small compressional peak, around 5 kHz, appears in the bending spectrum. The appearance of this peak is not an incorrect alignment of the coil or magnet, but a real physical effect called lateral inertia correction [1, 2]. Three measured peaks, corresponding to compressional, torsional and bending resonances, are given in detail in figure 6. Apart from the square of the acceleration (proportional to intensity $|\phi(z=0)|^2$), the corresponding phase $\theta(z=0)$ is given in the same figure. Lorentzian fits

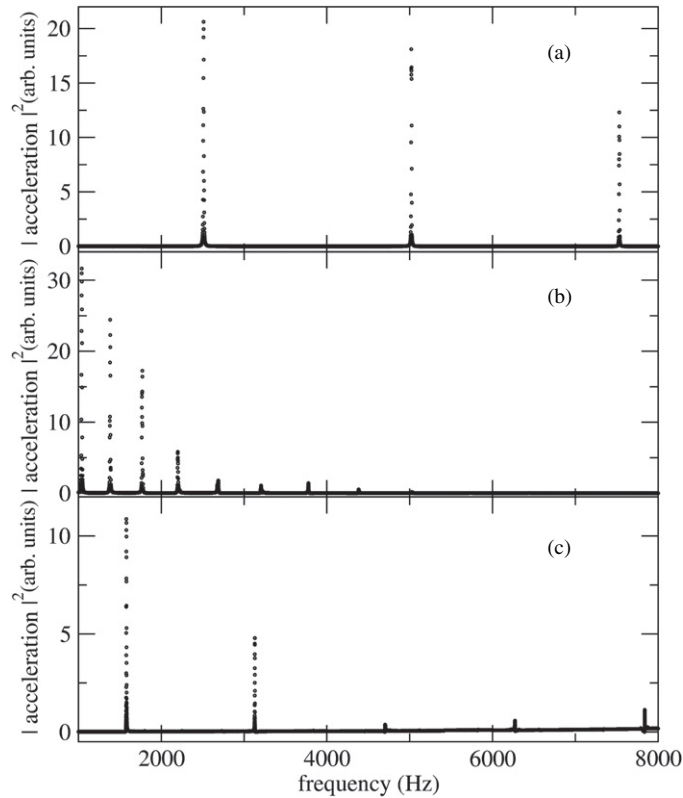


Figure 5. Measured spectrum using the setup of figure 3 and the EMAT configurations of figure 4. The aluminum rod is of length $L = 1$ m and has a circular cross-section of diameter $D = 1.27$ cm. (a), (b) and (c) correspond to compressional, bending and torsional spectra, respectively.

(see (12)) for the resonant peaks are also shown. The absorption parameter k_I can be obtained from the width of the fitted resonances. As can be seen in figure 6, the compressional and bending resonances are wider than the torsional. This is expected as the coupling of the torsional wave with the air is very small due to the circular symmetry of the cross-sectional area of the rod and the fact that shear waves cannot travel in air. As expected, the phase of the response shows a change of π for each resonance.

The velocity v of the compressional and torsional waves can be obtained by measuring several resonances as f_n are linear with n , and the slope is $v/2L$. In figure 7 the centers of the resonances as a function of n for torsional, compressional and bending waves are plotted. As can be seen in this figure, the bending waves are not linear with n ; this means that they are dispersive [2, 5]. The slopes of the curves for compressional and torsional waves yield wave speeds of $5\,025 \pm 5$ m s⁻¹ and $3\,135 \pm 1$ m s⁻¹, respectively. Note that the uncertainty for the compressional wave velocity is larger than that for the torsional waves; this is due to the Rayleigh or lateral inertia effect (see [2]). From these velocities some physical parameters of the aluminum rod can also be calculated. Using a value of $\rho = 2722 \pm 21$ Kg m⁻³, we obtained a Young's modulus $E = 68.6 \pm 0.3$ GPa from the compressional velocity and shear modulus $G = 26.7 \pm 0.2$ GPa. Those values agree with those found in the literature [8].

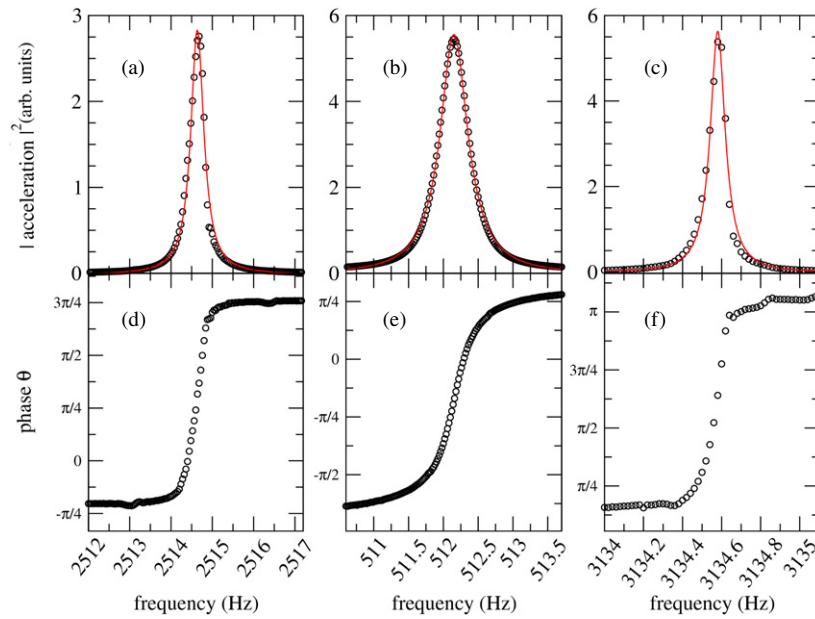


Figure 6. Measured resonances for the same rod of figure 5. The upper panels give the square of the acceleration and the lower panels the phase θ of the angle of twist. The solid (red online) lines correspond to Lorentzian fits (see equation 12) with parameters: (a) compressional $\Gamma = 0.39$ Hz and $f_r = 2514.6$ Hz; (b) bending $\Gamma = 0.49$ Hz and $f_r = 512.2$ Hz; and (c) torsional $\Gamma = 0.09$ Hz and $f_r = 3134.6$ Hz. Here f_r and Γ are the center and width of the Lorentzian fit, respectively.

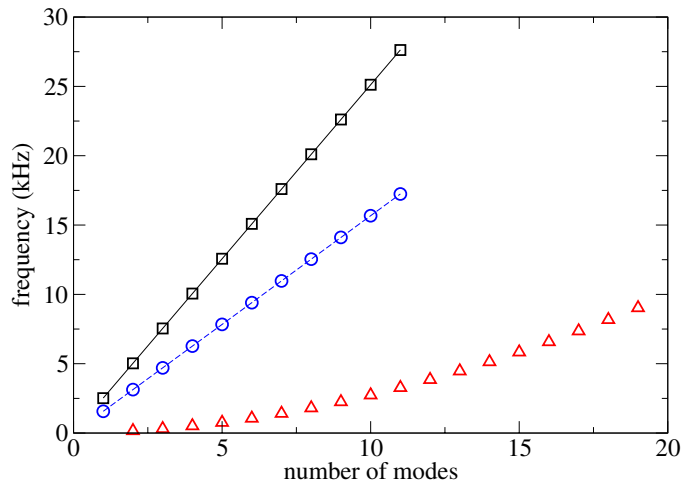


Figure 7. Resonant frequencies measured with the VNA and the EMATs for the same rod of figure 6 as a function of the number of modes. The results for compressional waves are given by squares (black), for torsional waves by circles (blue online) and for bending waves by triangles (red online). The solid and dashed lines correspond to a least-squares fit for the compressional and torsional results, respectively.

5. Conclusion

We have introduced an experiment for the advanced physics laboratory that permits undergraduates to learn the basic principles of spectroscopy. It also allows students to compare experimental results with theoretical predictions as very simple systems, such as a vibrating rod, can be studied both ways. The technique, called acoustic resonant spectroscopy, allows students to measure the resonant curve and the phase of the response.

This setup has a number of possible uses for undergraduate laboratory courses, since the rod can be substituted by arbitrary and more complicated elastic systems. Apart from being an experiment in which non-destructive testing can be performed, the apparatus can be used with great success to show interesting physical phenomena to students quantitatively; for example, the emergence of bands in periodic systems [9] and the wave amplitudes in plates with regular or irregular shapes [10], among many others. In fact, the effect of the absorption when covering part of the rod with an absorbing foam can also be studied; the width of the resonance curve for torsional waves was found to increase two orders of magnitude. We should also mention that the experimental setup had already been used successfully on three advanced physics laboratory courses.

Acknowledgments

We thank A Morales and E Basurto for their help in making the experimental measurements. We also thank X A Méndez-Báez, A Salas-Brito and A Arreola for useful comments. This work was supported by DGAPA-UNAM project IN11131 and by CONACYT project 79613.

References

- [1] Morales A, Gutiérrez L and Flores J 2001 *Am. J. Phys.* **69** 517
- [2] Graff K F 1975 *Wave Motion in Elastic Solids* (New York: Dover) pp 75–212
- [3] Rossing T D and Russell D A 1990 *Am. J. Phys.* **58** 1153
- [4] An illustrative animations of vibrations in rods is given in <http://www.fis.unam.mx/~mendez/animations.html>
- [5] Landau L D and Lifshitz E M 1976 *Theory of Elasticity* (Oxford: Pergamon) p 101
- [6] Crocker M J 1998 *Handbook of Acoustics* (New York: Wiley) p 681
- [7] Simpson H M and Wolfe P J 1975 *Am. J. Phys.* **43** 506
- [8] Crandall S H, Dahl N C and Lardner T J 1978 *An Introduction to the Mechanics of Solids* (Boston, MA: McGraw-Hill)
- [9] Morales A, Flores J, Gutiérrez L and Méndez-Sánchez R A 2002 *J. Acoust. Soc. Am.* **112** 1961–7
- [10] Flores J 2007 *Eur. Phys. J. S T* **145** 63–75